ELSEVIER

Journal of Nuclear Materials 306 (2002) 202–212

journal of nuclear materials

www.elsevier.com/locate/jnucmat

Raman microspectrometric identification of corrosion products formed on UO_2 nuclear fuel during leaching experiments

M. Amme [a,*], B. Renker [b], B. Schmid [c], M.P. Feth [c], H. Bertagnolli [c], W. Döbelin [d]

[a] *European Commission, Joint Research Centre, Institute for Transuranium Elements, Postfach 2340, D-76125 Karlsruhe, Germany*

[b] *Institute of solid state physics, Forschungszentrum Karlsruhe, Postfach 3640, 76021 Karlsruhe, Germany*

[c] *University of Stuttgart, Institute of Physical Chemistry, Pfaffenwaldring 55, D-70569 Stuttgart, Germany*

[d] *SVSMF Mineralogical Foundation Basel, Bündnerstr. 10, CH-4055 Basel, Switzerland*

Received 20 June 2002; accepted 24 September 2002

Abstract

The corrosion of directly disposed spent nuclear fuel by contact with intruding groundwater will alter the physical and chemical properties of this material. Secondary phases which formed during alteration of UO_2 surfaces were measured with Raman microspectrometry and the characteristic vibrational spectra of the materials were recorded. U phases were synthesized in hydrothermal autoclave syntheses. A Raman spectral library of UO_2 corrosion phases was set up for the identification of unknown products found on altered nuclear fuel samples. In a case study, U peroxide (UO_4) was identified by comparison with a natural sample as the main alteration phase by its characteristic O–O Raman vibration at 870 cm^{-1}. The results demonstrate the differentiation between UO_2 and its alteration products U(VI) oxyhydroxide and U(VI) peroxide (UO_4) on one sample with a relatively quick, non-destructive, spatially resolving measurement method which delivers oxidation state and molecular bonding information. Implications for the analysis of complex heterogenous matrices are discussed.

1. Introduction

Directly disposed high-level nuclear waste (like, in this present work, spent fuel) which is foreseen to be finally disposed in deep geological formations in many countries, consists of a variety of fission and activation products, long-lived actinides, and stable isotopes present in the matrix of the $^{238}UO_2$ material. Depending of the disposal concept, the spent nuclear fuel is stored within certain containments (steel, copper) with the aim to isolate the interior from the outside environment for about the first 1000 years [1]. Considering the scenario of eventual containment failure within geologic timescales, the knowledge of the chemistry of the solid-liquid interface, which controls the radionuclide release under these conditions, is important.

The formation of alteration products on nuclear fuel material exposed to chemically reactive repository components depends on the prevailing conditions. Parameters that control the amount and nature of the alteration products are, for instance, the pH and the Eh of the solution, the composition and ionic strength of the groundwater, the temperature, and the exposure time. Physical factors like the sample surface and surface

* Corresponding author. Tel.: +49-7247 951 148; fax: +49-7247 951 593.

E-mail address: amme@itu.fzk.de (M. Amme).

0022-3115/02/$ - see front matter
PII: S0022-3115(02)01291-6

roughness also play a role. Factors that have been considered in few investigations so far are, for example, the influence of organic matter, which is present in most groundwaters (either in the form of simple organic compounds, or as humic/fulvic compounds), and the presence of colloids, which might act as potential carriers for freshly forming crystals. Studies performed with UO_2 material under unsaturated test conditions (that is, a small liquid volume contacting a relatively big surface) and in oxic groundwater at 90 °C showed a preferential formation of schoepite during the first two years of the experiment, followed by the formation of uranyl silicates like uranophane and boltwoodite [2]. A more complex paragenetic sequence is observed when spent fuel is used for the experiments. Due to the presence of fission products, alteration phases were found to include rare earth elements (REE) like Ce, Sm, and Nd [3]. Uranyl oxihydroxide phases containing Cs and Mo were found in similar investigations [4]. It is not reported if radiolysis of the contacting water, induced by the strong radiation field present around fresh spent nuclear fuel, changed the alteration phase chemistry. A clear influence of water radiolysis products like H_2O_2 upon the surface development of leached nuclear fuel samples was observed in the case of simulated radiolysis experiments. Samples of UO_2 material, which were exposed to a high dose of alpha particles at the solid/liquid interface using a helium ion beam during the leaching experiment, developed a layer of uranium peroxide (UO_4, meta-studtite) on the surface [5]. Little is known about the reaction pathways and especially secondary phase chemistry of UO_2 alteration in anoxic conditions. Studies with natural analogue materials allow us to conclude that the chemistry of anoxic UO_2 alteration is governed by mechanisms like ion exchange, lattice incorporation and substitution in contrast to the reactions taking place under oxic conditions, where oxidative dissolution is the dominating mechanism [2]. In each case of repository conditions, solubility considerations play a major role for the assessment of storage safety of spent nuclear fuel.

The dissolution chemistry of actinides is strongly dependent on the prevailing redox conditions. In the case of uranium, in solid U phases the oxidation states IV and VI are encountered. Most investigations done so far were performed in oxic media and the redox state of resulting secondary products was therefore limited to +6. With both U(IV)/U(VI) phases present (as it is expected with spent fuel dissolving under repository vault conditions), an analytical method that is able to differentiate the U redox states of solids is needed. Raman vibrational spectroscopy can be used to record characteristic spectra of substances that possess unique vibrational bands characteristic for bonds in molecules or crystal lattices. The determination of oxidation states and the differentiation between chemically similar compounds is possible with this method. Furthermore, the technique can be used for microscale determinations, using a microscope accessory. Other advantages are that most samples need no special preparation, no vacuum has to be applied (which might lead to alteration or destruction of the sample). The characterisation of some natural (mineral) and synthetic U compounds (of very similar composition) with Raman spectroscopy and the derivation of their structures using the obtained information was described [6–8]. However, not all of the possible alteration phases resulting from the spent fuel corrosion were measured so far. Vibrational data of the U oxides containing U(IV) were obtained, allowing a differentiation of the oxides UO_2, U_3O_8, and U_4O_9 [9,10]. Some first attempts to characterise environmental U particles by comparison with standard Raman spectra were made [11], as well as the determination of the U oxidation state in an (artificially generated) mixture of U compounds [12]. More numerous examples are reported for the field of corrosion research using vibrational spectroscopy [13].

Modern spectral imaging techniques have broadened the field of applications in materials sciences. Since personal and laboratory computers are able to process high amounts of measured data, methods using spatially resolving spectrometrical measurements (generally known as 'mapping') were established for materials investigations. The resolution of Raman microspectrometry instruments is theoretically limited by the laser wavelength and reaches in practice the range of few μm. The advantage of this instrumentation is that simultaneously visual (optically obtained) and spectroscopical data of the measured sample surface can be compared and evaluated. The comparison of mechanical characteristics present on a surface with the intensity of features present in the spectrum of the same location allow conclusions of high significance. Raman chemical imaging spectroscopy proved to resolve particles of the anatase and rutile polymophs of TiO_2 in a mixture of the materials [14]. In an combined approach (using also IR and EDX spectroscopy), the determination of the Pu bonding state in heterogenous environmental samples by functional group analysis was demonstrated [15,16].

Knowledge of the surface composition of finally disposed spent fuel is a prerequisite for assessing the dissolution behaviour of the material. To provide this data, a method has to be found that can determine the complex phase assembly of relatively similar compounds that form on the surface of the material under final repository conditions. The present work demonstrates the applicability of Raman microspectrometry for such investigations by compiling a spectral database from synthetic and natural standard materials, ensuring thereby a quick and unambiguous identification of the surface products.

2. Experimental

2.1. Corrosion experiment

The formation of secondary phases on the surfaces of nuclear fuel samples (pellets of unirradiated UO_2) was induced with leaching experiments using as liquid phase de-ionized water spiked with concentrations of the water radiolysis product H_2O_2 in several concentration steps. The used concentrations of H_2O_2 (10^{-5}, 10^{-4}, 10^{-3}, 10^{-2} mol/l) were selected in agreement with the amounts of H_2O_2 which were measured in water previously irradiated with alpha particles [17]. The waters were spiked with diluted 30% H_2O_2 solution (Merck, p.a. grade) and contacted with pellets of UO_2 under argon atmosphere. The experiment was ended after 14 days of duration. In the case of the high oxidant concentrations, a yellow alteration layer was visible macroscopically on the originally black sample after 48 h. After ending the experiment, the solid and the liquid phase were separated by filtration with 450 nm filters.

2.2. Materials

Pellets of depleted UO_2 (weight per sample $\approx$1.2 g) were used as solid phase in the leaching experiments. The pellets were neither cut nor polished in order to keep a certain roughness in the surface structure which promotes the formation of solid precipitates during conduction of leaching experiments.

Before each experiment, the samples were annealed for 5 h at 1600 °C in a N_2/H_2 atmosphere in order to restore the stoichiometry of pure UO_2 as far as possible and to rule out the participation of U^{6+} ions in the leaching and oxidation process from the beginning.

2.3. Synthesis of UO_2 alteration products (uranium minerals)

Previous investigations, which were conducted both on corrosion of spent nuclear fuel [3,4] and naturally altered uraninite material (natural analogue) [18], were evaluated. Several uranium minerals were identified as possible alteration products, which can form on UO_2 surfaces as reported in previous work [19]. Materials, which represent typical alteration stages of nuclear fuel during contact with repository groundwater and degradation products, are uranyl oxihydroxides, -silicates, -carbonates, and uranyl minerals that contain one or more metal ions present in groundwater (alkaline or earth alkaline uranium compounds). During the oxidative dissolution of nuclear fuel, it was found in long-term experiments that the original matrix substance UO_2 is changed into several alteration products. The composition of these varies with the time duration of the experiment (shown in Fig. 1). This is a typical indicator for

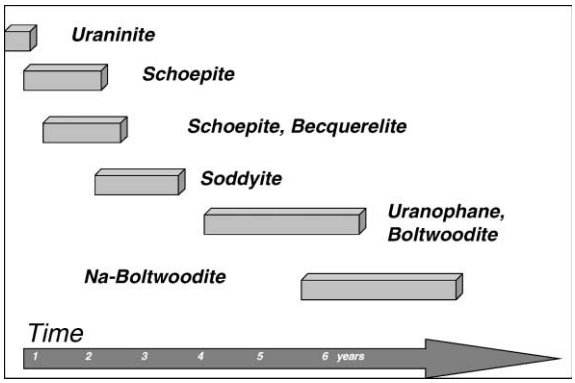

Fig. 1. Sequence of paragenetic mineral formation during oxidative alteration of UO_2 as observed experimentally by Wronkiewicz et al. [19]. The experiments were conducted in oxic atmosphere with a water containing all majour groundwater ions.

kinetically controlled formation processes. The U minerals compiled in Table 1 were found to appear frequently in these alteration sequences [19] and were therefore choosen for setting up a spectral database for the identification of nuclear fuel corrosion products.

Since the groundwaters contacting spent nuclear fuel after possible container corrosion and failure in the repository leakage scenario, contain a variety of ions, and mixed phases of uranium, ions like, e.g., Ca, K, Na, Si, CO_3^{2-} and others must be taken into account to appear in the UO_2 alteration sequence. Numerous minerals can be formed during these processes [26,27]. In this investigation, only phases that contain U, O and H were necessary for spectral identification of alteration products, since the experiments were conducted in de-ionized water and only hydrogen peroxide was added. However, several of the synthesized minerals will comprise the spectral library necessary for future investigations on

Table 1
Uranium minerals which were observed to form as alteration products of UO_2 corrosion during experiments simulating environmental conditions

Mineral	Formula	Reference
Coffinite	$USiO_4$	[20]
Becquerelite	$Ca[(UO_2)_6O_4(OH)_6] \cdot 8H_2O$	[21]
Schoepite	$(UO_2)(OH)_2 \cdot xH_2O$	[22,23]
Uranophane	$Ca(UO_2)SiO_3(OH)_2 \cdot 5H_2O$	Natural sample
Na-Boltwoodite	$(H_2O)Na(UO_2)(SiO_4)$	[24]
Soddyite	$(UO_2)_2SiO_4 \cdot 2H_2O$	[25]
Studtite	$UO_4 \cdot xH_2O$	Natural sample
Uraninite	UO_2	No special synthesis

samples corroded in groundwater. The uranium(IV) silicate was prepared to help in the identification of phases formed on UO_2 under anoxic conditions. About this we report elsewhere in detail [28].

Synthesis of the solids was performed by following the procedures reported by several authors. The appropiate amounts of uranyl nitrate ($UO_2(NO_3)_2$) of natural isotopic composition, Merck, p.a. grade) were dissolved in de-ionized water and mixed with solutions of the other reagents (Merck, p.a. grade). When the pH conditions of the acetate buffer were necessary, a calculated amount of acetic acid (Merck, p.a. grade) was added. When synthesis took place under hydrothermal conditions, teflon liners of 40 ml volume were used as reaction vessels and heated to reaction temperatures by an autoclave system. The pressures of the reacting solutions were not measured; they can be assumed to be approximately equal to the vapor pressure of water at the given temperatures (e.g., 15 bar. at 200 °C). After ending the synthesis, the products were filtered over glass filters and washed and cleaned according to the author's synthesis recommendations (using hot de-ionized water for the most cases). Table 2 summarizes the synthesis conditions. A synthesis of the mineral compreignacite ($K_2[(UO_2)_6O_4(OH)_6]\cdot 8H_2O$) was started but failed (schoepite was produced instead).

Natural samples of studtite (uranium peroxide) and uranophane from Menzenschwand, Germany (Black Forest) were used to complete the set of uranium standards. About 100 mg of the minerals were pulverized and analyzed for the impurity content with SEM-EDX prior to the experiments. The analysis proved a sufficient purity of the minerals.

2.4. SEM-EDX

Examination with SEM-EDX was performed with a Philips SEM 515 scanning electron microscope with an acceleration voltage of 30 kV, using a Tracor detector for the EDX measurements. The sample used for the corrosion experiment (UO_2 pellet) was placed on an aluminium cup sample holder and, thanks to the sufficiently high electrical conduction of UO_2, needed no noble metal coating. The synthetic U minerals are electrical insulators in most cases and were coated with Au prior to the SEM investigation.

2.5. NIR laser Raman spectroscopy measurements

Samples of the synthetic U(VI) phases were measured with a Bruker RFS 100/S Fourier Transform (FT) Raman spectrometer with attached Raman microscope (Nikon Optiphot-2 microscope) using an air-cooled near infrared (NIR) Nd:YAG laser with a wavelength of 1064 nm. Several mg of the materials were collected into a capillary glass tube and irradiated with laser light which had a power of 150 mW. The scattered light was collected with a high-sensitivity Ge diode (cooled with liquid nitrogen). For an average measurement, 128 scans were collected.

2.6. VIS laser Raman spectroscopy measurements

Samples of U(IV) phases and, for controlling the method, also U(VI) minerals, were measured with a Dilor XY Raman microspectrometer with attached microscope using an Ar laser with a wavelength of 514 nm. In practice, the spatial resolution of the scanning application reaches about 2 μm. A few mg of the materials were placed on an object slide under the Raman microscope and irradiated with laser light. In the case of corroded pellet samples, a suitable location was selected on the sample surface. For the U(VI) materials, an energy of 0.2 mW was used. The dark U(IV) materials absorb laser light much stronger and were irradiated with an energy of 20 mW in order to enhance the yield of the scattered light. Spectra were recorded with an liquid N_2 cooled silica detector (512 pixels).

Table 2
Conditions during synthesis of uranium solid phases and yield of products

Mineral	Conditions during synthesis	Yield (%)
Coffinite	pH 8.5 (sodium bicarbonate buffer), 30 days, 180 °C, starting substance UO_2 (powdered), SiO_2 gel (freshly precipitated from Na_2SiO_3) added	93.8
Becquerelite	pH 4.5 (actetate buffer), 30 days, 180 °C, starting substance $UO_2(NO_3)_2$, $CaCl_2$/HAc added	74.4
Schoepite	pH < 7, 14 days (aging), 25 °C, starting substance UO_2 $(NO_3)_2$, NaOH added	80.6
Uranophane	Natural sample	–
Na-Boltwoodite	pH basic, 30 days, 90 °C, starting substance $UO_2(NO_3)_2$, HAc/NaOH/Na_2SiO_3 added	71.3
Soddyite	pH 5 (actetate buffer), 7 days, 140 °C, starting substance $UO_2(NO_3)_2$, HAc and SiO_2 (powdered) added	28.3
Studtite	Natural sample	–
Uraninite	UO_2	No special synthesis

3. Results and discussion

During the experiment, the solid samples were occasionally examined optically and showed a different behaviour. Samples containing the highest concentration of oxidant showed a pale yellow discolouration on their surfaces, which is interpreted as the formation of a layer or coating. The samples that were contacted with solutions containing 10^{-3} M H_2O_2 showed the same behaviour, but the alterations were much less visible. All other samples showed no visible alterations.

Examination with scanning electron microscopy showed that the pellets changed their surface structure, and, partly, suffered severe surface damage. At the highest H_2O_2 concentrations, an amorphous layer, which was disturbed by cracks, covered the complete surface. The original grain boundary structure of the UO_2 was no longer visible. Fig. 2 shows a SEM image of the specimen that was corroded in the solution containing the highest oxidant concentration. All observed phases were examined with EDX analysis for the elemental composition. No other elements besides uranium were found. Since the configuration of the instrumental technique does not allow to detect elements with a smaller atomic order number than that of sodium (=12), the presence of relatively light elements like C cannot be ruled out. The presence of oxygen in the measured phases was assumed.

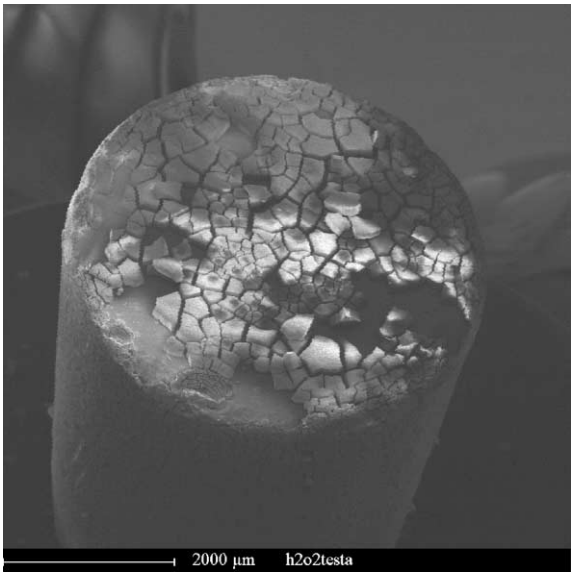

Fig. 2. SEM image of a UO_2 sample corroded after exposure to a solution containing H_2O_2 (simulated radiolysis experiment) The sample is about 6 mm in diameter.

3.1. Compilation of a spectral library for uranium phases: measurement with a NIR Raman spectrometer

Spectra of the synthesized uranium compounds were recorded in order to set up the Raman spectral library before examining the unidentified alteration materials on the corroded samples. Measurements of the synthetic phases were performed with a near infrared (NIR) and a visible light (VIS) laser. In the case of the NIR-FT Raman measurements, the U(VI) compounds (mostly yellow in colour) yielded spectra with good scatter intensities, due to their high reflectivity. The darkly coloured U(IV) compounds (UO_2 and $USiO_4$) absorbed the NIR light very strongly, which resulted in spectra of poor quality. The bad signal-to-noise ratio of their NIR spectra made an evaluation impossible. However, other workers reported previously about successful IR spectroscopy measurements on these substances [9,29].

The uranium(VI) compounds delivered spectra that show similar features. In each case, a signal is present in the vicinity of 800 cm^{-1}, resulting from the symmetric axial stretch vibration of the uranyl ion. This signal varies in its position in the spectrum, depending on the bonding situation of the uranyl group in the solid [30]. Generally, a shift of the Raman peak to higher wavenumbers in the spectrum is observed when lighter elements take part in the bond. Some minor signals are visible around 500 and 300 cm^{-1}, resulting from equatorial U–O stretch vibrations and U–O bending modes, respectively (Si–O vibration are found in this area also). These signals are not as well identificable as the strong U–O vibration, and can therefore serve only as additional information on the chemical state of the substance. A detailed analysis of recorded spectra and a prediction of expected spectra could be performed by the means of a symmetry group analysis. We dispensed with such a theoretical analysis here since the identification of unknown substances by spectra comparison is sufficient for qualitative speciation. Symmetry group discussions of the vibrational modes of UO_2 and other fluorite-structure compounds can be found in other works [31–33].

Raman measurements of some of the substances measured in this work were reported previously. These results are compared with the present work later in Table 3.

The schoepite spectrum (Fig. 4(b)) shows a typical double peak which results from the uranyl ion being present in two non-equivalent sites [6–8]. The position of this double peak can change in the spectrum depending from the degree of hydration of the substance; the value found here, 843 cm^{-1}, is in excellent agreement with previous values for the same material [7]. The symmetric stretch modes of boltwoodite (Fig. 4(a)) and soddyite (Fig. 4(d)) were found at 839 and 830 cm^{-1}, respectively; the one for natural uranophane (Fig. 4(c)) at 793 cm^{-1}.

Table 3
Summary of the characteristic wavenumbers measured for the substances used in this work and comparison with Raman and IR reference data

Mineral	Formula	Measured wavenumbers (this work) (cm^{-1})	Wavenumber acc. to reference (cm^{-1})
Coffmite	$USiO_4$	ν(U–O ?):970 ν(Si–O ?):1154	– (analogue $ZrSiO_4$: ν(Si–O ?):1248)
Na-Boltwoodite	$(H_2O)Na(UO_2)(SiO_4)$	$\nu_1(UO_2^{2+})$:839 $\nu_3(SiO_4^{4-})$:954	$\nu_1(UO_2^{2+})$:796 $\nu_3(SiO_4^{4-})$:965 (R, [6])
	$Na(UO_2)(SiO_3OH)\cdot H_2O$		$\nu_1(UO_2^{2+})$:780 $\nu_3(UO_2^{2+})$:880 $\nu_3(SiO_4^{4-})$:940 (IR, [37])
Soddyite	$(UO_2)_2SiO_4\cdot 2H_2O$	$\nu_1(UO_2^{2+})$:830 $\nu_2(UO_2^{2+})$:220, 259 $\nu_2(SiO_4^{4-})$:455	$\nu_2(SiO_4^{4-})$:457 $\nu_1(UO_2^{2+})$:824 (R, [6])
			$\nu_1(UO_2^{2+})$:832 $\nu_2(UO_2^{2+})$:228,268 $\nu_2(SiO_4^{4-})$:474 (IR, [37])
Uranophane	$Ca(UO_2)_2(SiO_3OH)_2\cdot 5H_2O$	$\nu_1(UO_2^{2+})$:793 $\nu_2(SiO_4^{4-})$:459 $\nu_3(SiO_4^{4-})$:986	$\nu_1(UO_2^{2+})$:797 $\nu_3(SiO_4^{4-})$:970 (R, [6])
			$\nu_1(UO_2^{2+})$:790 $\nu_2(SiO_4^{4-})$:460 $\nu_3(SiO_4^{4-})$:942 (IR, [38])
Studtite	$UO_4\cdot 4H_2O$	$\nu_1(UO_2^{2+})$:820 $\nu(O_2^{2-})$:870	$\nu_1(UO_2^{2+})$:820 $\nu(O_2^{2-})$:875 (IR, [39])
Becquerelite	$Ca[(UO_2)_6O_4(OH)_6]\cdot 8H_2O$	$\nu_1(UO_2^{2+})$:828	$\nu_1(UO_2^{2+})$:841 (R, [8])
			$\nu_1(UO_2^{2+})$:810 (IR, [40])
Schoepite	$[(UO_2)_8O_2(OH)_{12}](H_2O)_{12}$	$\nu_1(UO_2^{2+})$:843/855 (double peak)	$\nu_1(UO_2^{2+})$:840/860 (double peak), (R, [41])
			$\nu_1(UO_2^{2+})$:844 (R, [8]), $\nu_1(UO_2^{2+})$:846 (R, [7]), $\nu_1(UO_2^{2+})$:842 (R, [6])
Uraninite	UO_2	Unknown:369 $\nu_1(T_{2g})$:445	$\nu_1(T_{2g})$:445 (R, [9])

IR: Infrared measurements.
R: Raman measurements.
$\nu_1(UO_2^{2+})$: symmetric stretching vibration of uranyl (in symmetric Uranyl-Ions: Raman active, IR inactive; with reduction of symmetry IR active, also).
$\nu_2(UO_2^{2+})$: bending vibration (↻) of uranyl.
$\nu_3(UO_2^{2+})$: antisymmetric stretching vibration (in symmetric Uranyl-Ions: IR active, Raman inactive; with reduction of symmetry Raman active, also).
Free SiO_4^{4-}-anions: $\nu_1(A_1,SiO_4^{4-})$:819 cm^{-1} (Raman active), $\nu_2(E,SiO_4^{4-})$: 340 cm^{-1} (Raman active), $\nu_3(F_2,SiO_4^{4-})$: 956 cm^{-1} (Raman + IR active), $\nu_4(F_2,SiO_4^{4-})$: 527 cm^{-1} (Raman + IR active).

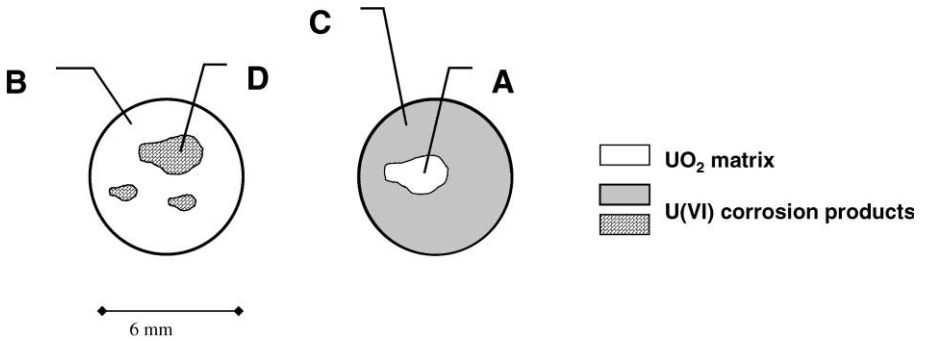

Fig. 3. Locations on the sample surfaces where Raman spectra were collected. Both circles (sample surfaces) are about 6 mm in diameter. Left sketch: sample corroded in 10^{-2} M H_2O_2. Right sketch: sample corroded in 10^{-3} M H_2O_2. The spectra designated by the measurement points (A,B,C,D) are displayed in Fig. 6(a)–(d) and are discussed in the text.

Literature values differ slightly from these data, which might be due to compositional differences. However, the composition of the synthetic minerals used in this work is supported additionally by their acicular crystal shape and their U-Si ratio, as determined with SEM-EDX, and an additional typical Raman signal around 950 cm^{-1} [7]. Signals in some of the spectra found at about 1000 cm^{-1} are supposed to stem from unreacted SiO_2 which could not be removed totally after the synthesis steps.

3.2. Measurement with a VIS laser Raman spectrometer

The dark samples consisting of U(IV) compounds were measured with an Ar laser (514 cm^{-1}) to avoid the strong absorption effect of dark material in IR light. Reasonable spectra could be obtained by using this technique. No significant fluorescence disturbed the recording of the spectra. In a first step, the capability of the method to obtain the desired information was tested

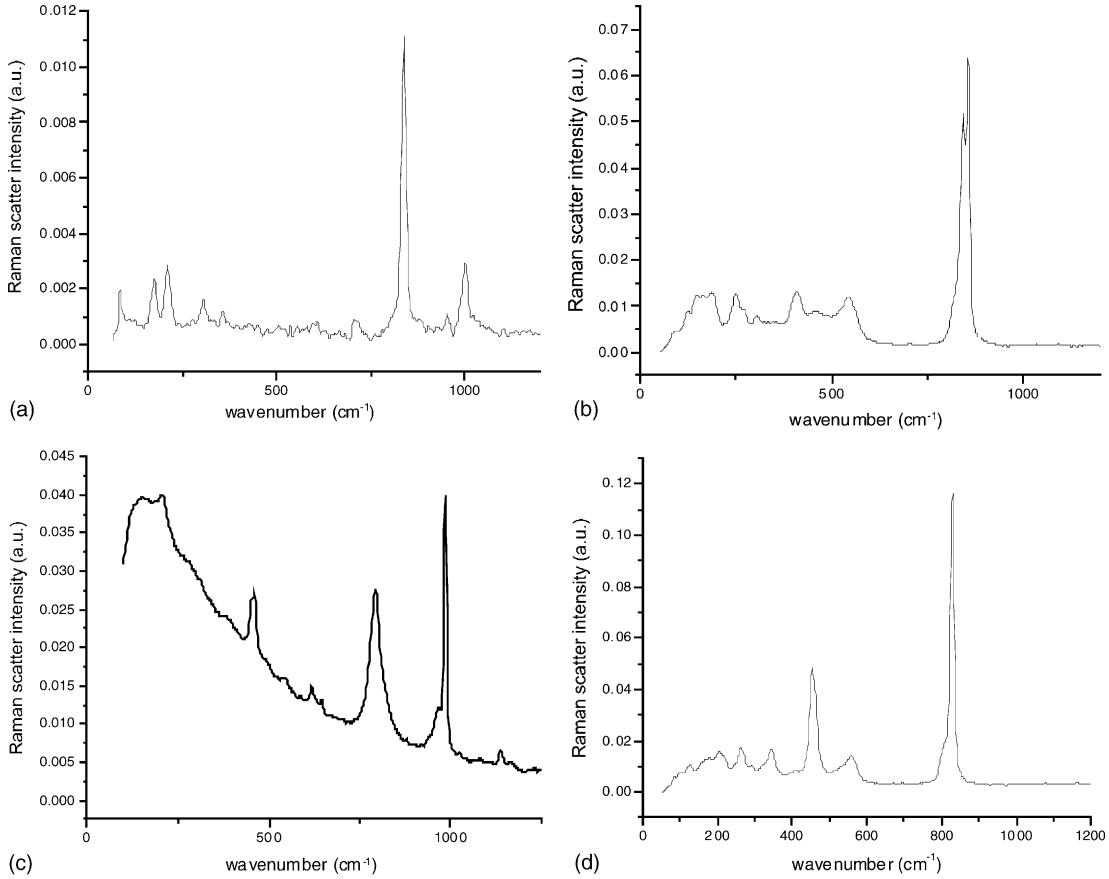

Fig. 4. (a) Raman spectrum of synthetic boltwoodite ($(H_2O)Na(UO_2)(SiO_4)$), measured with laser light of a wavelength of 1064 nm. (b) Raman spectrum of synthetic schoepite ($(UO_2)(OH)_2 \cdot xH_2O$), measured with laser light of a wavelength of 1064 nm. (c) Raman spectrum of natural uranophane ($Ca(UO_2)SiO_3(OH)_2 \cdot 5H_2O$), measured with laser light of a wavelength of 1064 nm. (d) Raman spectrum of synthetic soddyite ($(UO_2)_2SiO_4 \cdot 2H_2O$), measured with laser light of a wavelength of 1064 nm.

by measuring a powdered sample of the matrix material UO_2. The resulting spectrum had an intensity sufficient for further evaluation; it showed the typical U–O signals at the position reported by former investigators (see Table 3) [9,10]. The peaks found for the UO_2 oxidation product U_3O_8 between 700 and 800 cm^{-1} [10] could not be detected (Fig. 5(a)).

The synthetic U(IV) silicate (coffinite, Fig. 5(b)) shows a strong Raman signal at 1150 cm^{-1}; the fingerprint signals of the synthesis educt substance UO_2 (at 445 cm^{-1} are hardly visible as a peak anymore, proving therefore that the synthesis has proceeded until a satisfactory degree. The signal found for coffinite could be interpreted as a silicate vibration; this hypothesis is supported by the fact that zircon ($ZrSiO_4$) shows its major Raman vibrational signal at 1248 cm^{-1}. The IR spectra of both substances show strong similarities [29]. The Raman vibrational spectra are, due to the isostructural crystal type of $ZrSiO_4$ and $USiO_4$, supposed to be very similar, also. As far as known, the minerals coffinite and studtite were measured for the first time in the present work with this technique.

In addition to the dark samples, some of the coloured U(VI) phases were measured with the Ar laser Raman equipment to have direct comparison of the two systems using different measuring wavelengths. Schoepite was measured with the 514 nm equipment to have a comparison of the results delivered by the two methods. The Raman spectrum obtained by this method delivered the major signal at 843 cm^{-1} and hence shows agreement with the NIR result. Synthetic becquerelite (Fig. 5(c)) was measured to have the dominant signal at 833 cm^{-1}, a value which is, however, in some contrast to the reported literature value of 841 cm^{-1} [8]).

3.3. Measurement of corroded samples and comparison with synthetic standard spectra

Samples corroded in solutions containing 10^{-3} and 10^{-2} M H_2O_2 were found to be coated by optically vis-

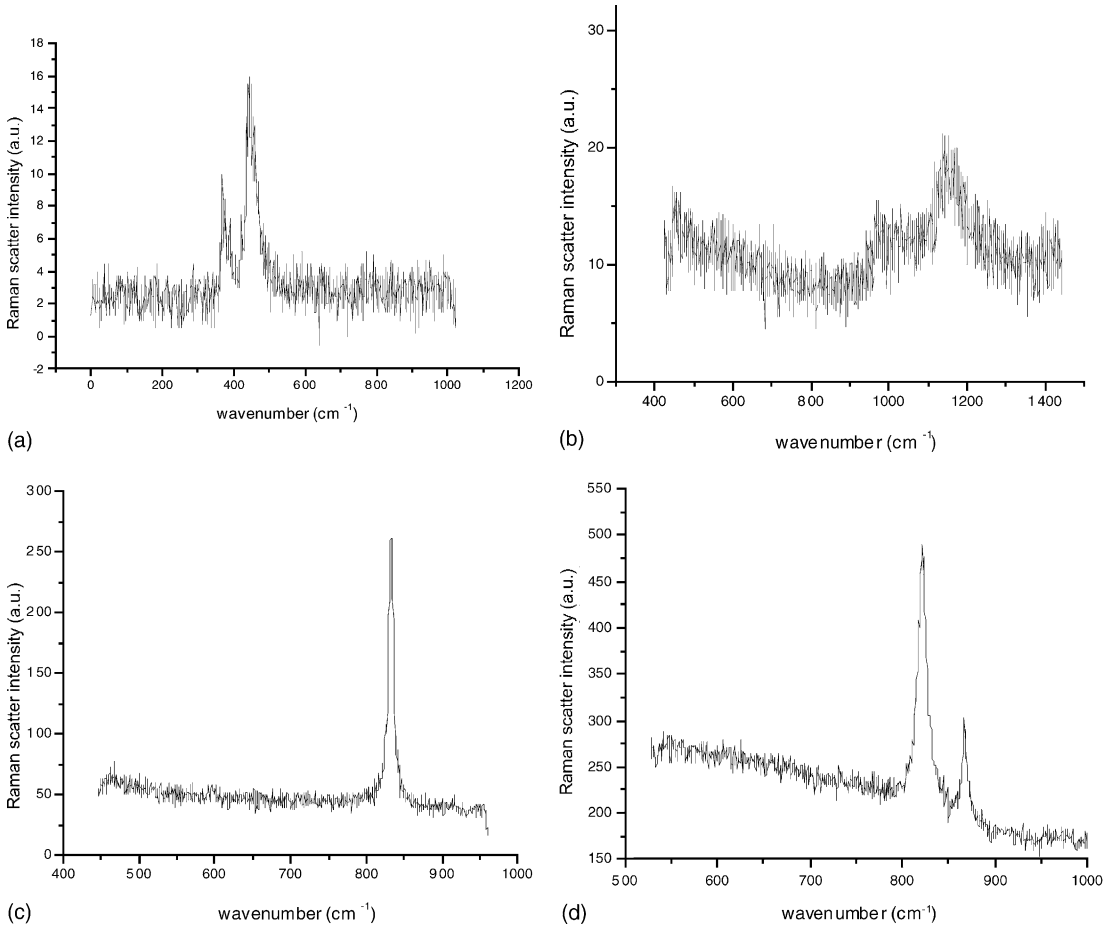

Fig. 5. (a) Raman spectrum of UO_2, recorded using a 514 nm VIS laser (b) Raman spectrum of synthetic coffinite ($USiO_4$), recorded using a 514 nm VIS laser (c) Raman spectrum of synthetic becquerelite ($Ca[(UO_2)_6O_4(OH)_6] \cdot 8H_2O$), recorded using a 514 nm VIS laser (d) Raman spectrum of natural studtite ($UO_4 \cdot xH_2O$), recorded using a 514 nm VIS laser.

ible corrosion layers and were therefore the first specimen selected for Raman microspectrometric measurements. Under the optical microscope, a clear separation between coloured areas (locations covered with alteration phases) and grey-black areas (unaltered UO_2 matrix) was observed. Spectra were recorded repeatedly at different selected points of both areas (points A,B,C and D as shown in Fig. 3).

Spectra which were collected from the unaltered matrix material on the selected samples showed similar characteristic features. In all these spectra (shown in Fig. 6(a) and (b)), the U–O vibration signal at 450 cm^{-1} was present, identifying the material as UO_2 [9,12]. Spectra from the yellow areas (Fig. 6(c) and (d)) contained a strong signal at 817 cm^{-1}, which was expected and is typical for the uranyl U–O vibration, as it was often observed in that wavenumber range when measuring the synthetic standards. The spectra show the additional feature of a vibration appearing at 870 cm^{-1} which is not present in any of the synthetic standard materials. A comparison with the Raman spectrum of potassium peroxide shows that the O–O vibration of the peroxide group of this substance appears at 890 cm^{-1} [30]. Other peroxides reveal signals of the O–O group in the same area (Sr peroxide: 860 cm^{-1}, Zn peroxide: 835 cm^{-1} [34]). It is therefore assumed that the signal found at 870 cm^{-1} has its origin in the O–O vibration of uranium peroxide (which has the half-structural formula UO_2–O_2).

The Raman spectrum of studtite (Fig. 5(d)) can hence be recognized uniquely from that of other uranyl compounds. The spectrum of the corrosion phase shows clear differences from the spectrum of schoepite (which is often observed in nuclear fuel corrosion experiments as an alteration phase [35]).

The Raman spectrum, recorded from a natural sample of studtite (Fig. 5d), shows two major signals at 823 and at 869 cm^{-1}, thereby identifying the corrosion

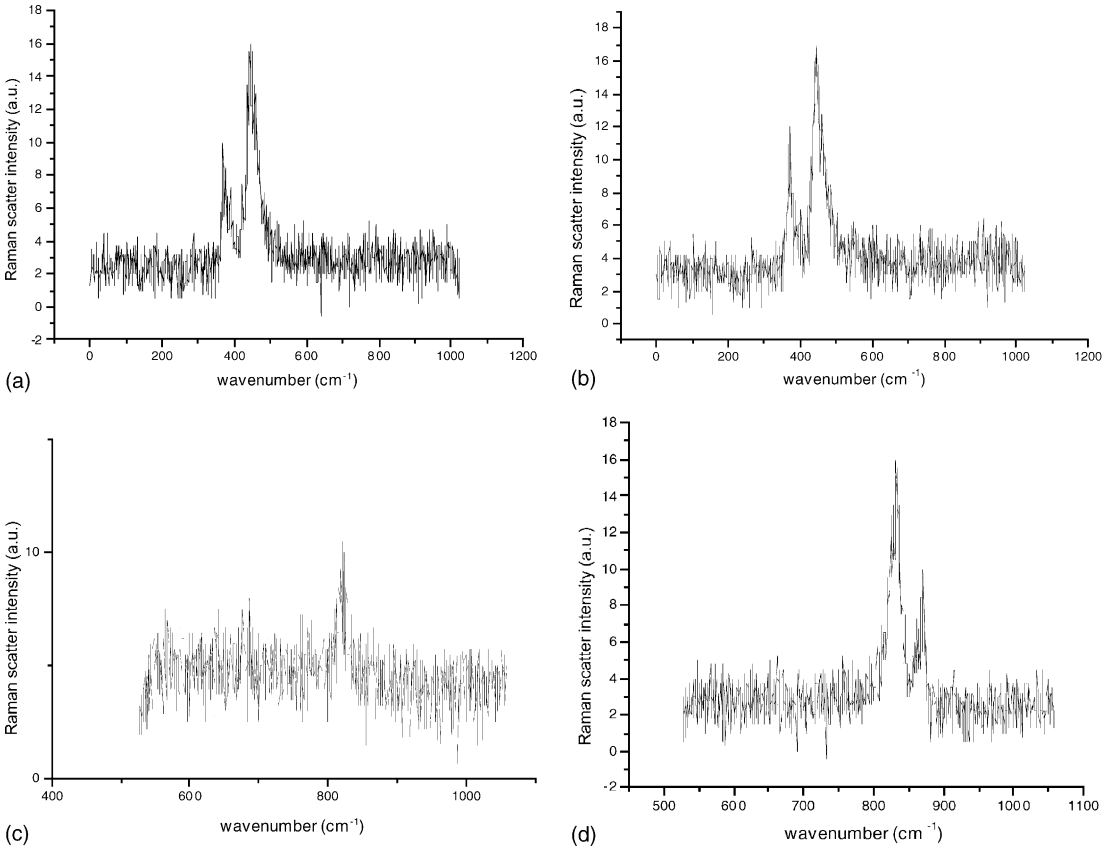

Fig. 6. (a) Raman spectrum of the UO_2 matrix material of the sample treated in water containing 10^{-3} mol/l H_2O_2 (point 'A' in Fig. 3) (b) Raman spectrum of the UO_2 matrix material of the sample treated in water containing 10^{-2} mol/l H_2O_2 (point 'B' in Fig. 3) (c) Raman spectrum of the corrosion phase of the sample treated in water containing 10^{-3} mol/l H_2O_2 (point 'C' in Fig. 3) (d) Raman spectrum of the corrosion phase of the sample treated in water containing 10^{-2} mol/l H_2O_2 (point 'D' in Fig. 3).

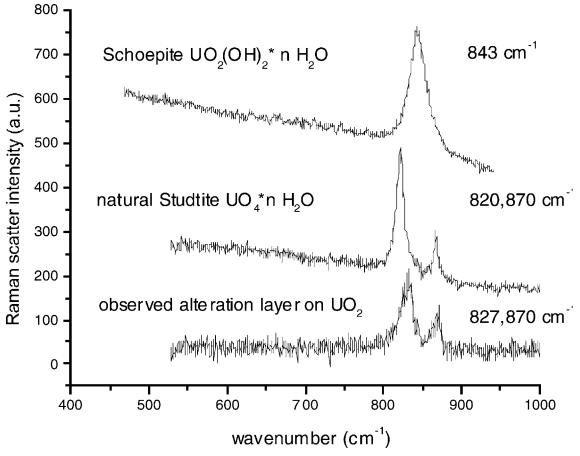

Fig. 7. Comparison of the Raman spectra of the corroded sample surface and the synthetic standards (compounds containing U, O and H). The single peak of the U–O vibration of schoepite cannot be found in the surface spectrum anymore, whereas the U–O and O–O vibrations of studtite are easily identified.

layer on the surface of the experimental specimen as studtite phase. This is shown in Fig. 7. A slightly broader signal of the U–O vibration in the spectrum of the natural sample is possibly caused by the presence of further uranyl phases in minor quantity. A measurement of the corroded area with a spatially resolving mode (often referred to as 'mapping') would give information about the extent of these phase mixtures [36]. This was not performed in this work.

4. Considerations concerning the geochemical speciation of elements present in spent nuclear fuel

The presence of the oxidant hydrogen peroxide leads the corrosion of nuclear fuel material into directions that are different from the normal pathways of oxidative dissolution. The formation of uranium peroxide was observed under laboratory conditions during radiolysis experiments [5], as well as having taken place in nature [26]. In the latter case it can be considered to be a

relatively rare phenomenon of uraninite alteration. Still, it can be expected to contribute to the alterations which spent nuclear fuel might suffer when this material possibly comes into contact with repository groundwater and degradation products after a certain time of final storage. This assumes that a strong radiation field is generated by the decaying nuclides. The substances that might form out of the reactions of UO_2 in a de-ionized aqueous system are limited in their composition (mainly U(VI) oxyhydroxydes and U peroxides are expected, as well as mixed U(IV)–U(VI) oxides). Still, numerous phases of different compositions can result in such a system, depending from the reaction conditions [8,19,42,43], as shown in the present experiments. The solid state speciation of these compounds, which are relatively similar in composition and structure, is not trivial. Raman microspectroscopy constitutes a method that can deliver information about the bonding situation in substances composed of the same elements (complementing SEM-EDX information); it is applicable for amorphous thin layers as they were observed in the experiments performed here (enhancing the information gathered with XRD); and it does not necessarily change the sample environment during the measurement. This latter effect must be considered when applying techniques which operate in vacuum.

Fission product elements and transuranic actinides are likely to be present in the alteration chemistry of the solid/liquid interface of disposed nuclear fuel after an assumed contact with water. They are present in freshly discharged spent nuclear fuel in a variety of crystalline, amorphous and metallic phases [44]. It can be expected that in parallel to the formation of alteration phases on the surface of the UO_2 matrix, an alteration phase chemistry of these elements will take place. The expected mechanisms are incorporation into uranium secondary minerals or separate phase formation. Such participation of further elements was observed in laboratory experiments [19], as well as in the case of natural analogue materials [45]. Depending from the geochemical conditions which prevail in the repository (for example pH, Eh, and concentration of ions like Si, Ca or carbonate), reactions with the ions present in groundwater are expected also. Many of the U compounds which result from transformations involving these ions are well investigated, but similar knowledge about transuranics compound formation (e.g., Pu or Np phases) is almost missing. Detailed examination of these phases would be advantageous in order to provide a base for the discussion of spent fuel corrosion behaviour after a possible assumed contact with intruding groundwaters. Raman spectroscopy provides a useful method to characterize these complex secondary products. Future investigations in which it is planned to use actual spent fuel samples and actinide compounds are projected in that direction.

5. Conclusions

The possibility to use a microscopic, spatially resolving scanning application, combined with the software-based identification of the numerous possible fission product secondary materials using a spectral library, seems especially promising for the further investigation of the complex, heterogenous chemical system which is present in spent nuclear fuel corrosion processes.

The findings in our work allow us to conclude the following:

1. Uranium peroxide (UO_4) is the major phase present on samples of the simulated radiolysis experiment. Its Raman spectrum is almost identical with that of natural studtite (which was most obviously formed by natural water radiolysis). Almost no schoepite or other uranyl oxyhydroxide was detected on the surface of the specimen (very weak lines typical for the schoepite vibration were observed).
2. The alteration material is clearly distinguishable from the UO_2 matrix by its features in the Raman spectrum. The Raman microprobe setup allows separate detection of corrosion particles and matrix material that are associated in an area of square-μm dimensions.
3. The examined material can be specified from other very similar U(VI) compounds, since every uranyl compound shows the U–O stretch signal at a unique position in the spectrum, due to the bonding situation in the molecule. This finding is important for the solid speciation of samples that were generated in an environment with complex chemistry (e.g., corrosion in the presence of groundwater and mineral phases).
4. The sample needs no special preparation and the measurements were performed on an area of square μm in a spatially resolving mode. Care must be taken, however, to minimize the applied laser power as far as possible, to avoid sample oxidation.
5. The preparation of a spectral library (using standard substances) is useful for the examination of systems in which several quite similar solid phases can be formed. This is expected, for example, in the case of experiments on spent fuel alteration in the presence of groundwater, barrier materials or enviromental substances.

Acknowledgements

The authors acknowledges Dr Ian Ray, Dr Thierry Wiss and Mr Hartmut Thiele for help with the SEM imaging technique and Mr Wolfgang Schmitt for supporting us with additional micromount mineral specimens for comparison.

References

[1] W. Miller, R. Alexander, N. Chapman, I. McKinley, J. Smellie, Geological disposal of radioactive wastes & natural analogues, Waste management Series vol. 2, Pergamon/Elsevier, 2000.

[2] D. Wronkiewicz, J. Bates, S. Wolf, E. Buck, J. Nucl. Mater. 190 (1992) 107.

[3] P. Finn, J. Bates, J. Hoh, J. Emery, L. Hafenrichter, E. Buck, M. Gong, Mat. Res. Soc. Symp. Proc. 333 (1994) 399.

[4] E. Buck, D. Wronkiewicz, P. Finn, J. Bates, A new uranyl oxide hydrate phase derived from spent fuel alteration, J. Nucl. Mater. 249 (1997) 70.

[5] G. Sattonay, C. Ardois, C. Corbel, J. Lucchini, M.-F. Barthe, F. Garrido, D. Gosset, Alpha-radiolysis effects on UO_2 alteration in water, J. Nucl. Mater. 288 (2001) 11.

[6] B. Biwer, W. Ebert, J. Bates, J. Nucl. Mater. 175 (1990) 188.

[7] H. Hoekstra, S. Siegel, J. Inorg. Nucl. Chem. 35 (1973) 761.

[8] R. Sobry, J. Inorg. Nucl. Chem. 35 (1973) 2753.

[9] G. Allen, I. Butler, N. Tuan, J. Nucl. Mater. 144 (1987) 17.

[10] I. Butler, G. Allen, N. Tuan, Appl. Spectr. 42 (5) (1988) 901.

[11] D. Morris, P. Allen, J. Berg, C. Chisholm-Brause, S. Conradson, R. Donohoe, N. Hess, J. Musgrave, C. Tait, Env. Sci Technol. 30 (1996) 2322.

[12] F. Purcell, H. Etz, in: K. Heinrich (Ed.), Microbeam Analysis–1982, San Francisco Press, San Francisco, 1982, p. 301.

[13] J. Maslar, W. Hurst, W. Bowers, J. Hendricks, J. Nucl. Mater. 298 (2001) 239.

[14] M. Schaeberle, H. Morris, J. Turner II, P. Treado, Analytical Chemistry News and Features, March 1 (1999) 175.

[15] J. Schoonover, F. Weesner, G. Havrilla, M. Sparrow, P. Treado, Appl. Spectr. 52 (1998) 1505.

[16] J. Schoonover, A. Saab, J. Bridgewater, G. Havrilla, C. Zugates, P. Treado, Appl. Spectr 54 (2000) 1362.

[17] S. Sunder, D. Shoesmith, N. Miller, J. Nucl. Mater. 244 (1997) 66.

[18] D. Zhao, R. Ewing, Radiochim. Acta 88 (2000) 739.

[19] D. Wronkiewicz, J. Bates, S. Wolf, E. Buck, J. Nucl. Mater. 238 (1996) 78.

[20] C. Keller, Über die Festkörperchemie der Actiniden-Oxide, Kernforschungszentrum Karlsruhe KfK-Report 225, (1964).

[21] J. Protas, Bull. Soc. Franc. Mineral. Crist. 82 (1959) 239.

[22] A. Sandino, B. Grambow, Radiochim. Acta 66&67 (1994) 37.

[23] J.M. Peters, Mem. Soc. Roy. Sci. Liege [5] 14 (1967) 5.

[24] R. Vochten, N. Blaton, O. Peters, K. van Springel, L. van Haverbeke, Can. Mineral. 35 (1997) 735.

[25] H. Nitsche, H. Moll, G. Schuster, G. Bernhard, E. Brendler, W. Matz, J. Nucl. Mater. 227 (1995) 40.

[26] R. Gaines, H. Skinner, E. Foord, A. Rosenzweig, Dana's New Mineralogy, 8th Ed., John Wiley, New York, 1997.

[27] M. Robault, Les minerais uraniferes francais et leurs gisement, Saclay, 1960.

[28] M. Amme, Appl. Geochem. (in preparation).

[29] L. Fuchs, H. Hoekstra, The American Mineralogist 44 (1959) 1057.

[30] J. Weidlein, U. Müller, K. Dehnicke, Schwingungsspektroskopie, Georg Thieme, Stuttgart, 1988.

[31] V. Keramidas, W. White, J. Chem. Phy. 59 (1973) 1561.

[32] M. Ishigame, M. Kojima, Journal of the Physical Society of Japan 41 (1976) 202.

[33] S. Kern, C. She, Chem. Phys. Letters 25 (1974) 287.

[34] R. Nyquist, C. Putzig, M. Leugers, Infrared and Raman Spectral Atlas of Inorganic Compounds and Organic Salts: Raman Spectra, vol. 2, Academic Press, San Diego, 1977.

[35] Hj. Matzke, J. Nucl. Mater. 238 (1996) 58.

[36] L. Sangaletti, L. Depera, B. Allieri, F. Pioselli, E. Comini, G. Sberveglieri, M. Zocchi, J. Mater. Res. 13 (9) (1998) 2457.

[37] S. Gevorkyan, A. Matkovskiy, A. Povarennykh, G. Sidorenko, Mineral Zh. Kiev 1 (1979) 78.

[38] J. Cejka, in: P. Burns, R. Finch (Eds.), Uranium: Mineralogy, Geochemistry and the Environment, Reviews in Mineralogy, vol. 38, Mineralogical Society of America, Washington D.C., 1999.

[39] J. Cejka, J. Sejkora, M. Deliens, Nues JB Miner. Mh. 3 (1996) 125.

[40] J. Cejka, J. Sejkora, M. Deliens, Neues JB Miner. Abh. 174 (1998) 159.

[41] L. Maya, G. Begun, J. Inorg. Chem. 43 (1981) 2827.

[42] D. Smith, B. Scheetz, Uranium 1 (1982) 79.

[43] P. Burns, R. Finch, (Eds.), Uranium: Mineralogy, Geochemistry and the Environment, Reviews in Mineralogy, vol. 38, Mineralogical Society of America, Washington D.C., 1999.

[44] H. Kleykamp, J. Nucl. Mater. 131 (1985) 221.

[45] J. Janeczek, R.C. Ewing, V.M. Oversby, L.O. Werme, J. Nucl. Mater. 238 (1996) 121.